3D-Printed Reinforcers for Shelves in Panel Furniture Fabricated from Polyamide Filament

Chen Wang,[a,b,*] Hanyi Huang,[a] and Jiahao Yu [b]

To address the issue of bending deformation in panel furniture shelves under prolonged loading, this study developed a 3D-printed shelf reinforcer using polyamide 6 (PA6) filament *via* fused filament fabrication (FFF) technology. Initially, the bending performance of PA6 models was analysed under varying process parameters (infill structure, infill thickness, and extrusion flow rate) using the three-point bending method. Subsequently, the reinforcer was custom designed and 3D-printed according to the target shelf's actual dimensions. Experimental results indicated that, among the three infill structures, the honeycomb infill structure exhibited the best bending performance, followed by the grid infill structure, and the line infill structure performed the worst. As infill thickness and extrusion flow rate increased, the bending performance of PA6 models progressively improved. The shelf reinforcer, 3D-printed with a honeycomb infill structure, 1.2 mm infill thickness, and 12 mm³/s extrusion flow rate, exhibited superior surface quality and achieved a tight fit with the shelf. This reinforcer effectively enhanced the shelf's bending performance and load-bearing capacity, extending the furniture's service life and providing practical reference for the rapid development of similar household items.

DOI: 10.15376/biores.21.1.799-807

Keywords: Fused filament fabrication; 3D printing; Shelf reinforcer; Polyamide filament

*Contact information: a: College of Furnishings and Industrial Design, Nanjing Forestry University, Nanjing 210037, China; b: Jiangsu Co-Innovation Center of Efficient Processing and Utilization of Forest Resources, Jiangsu, China; *Corresponding author: 996869559@qq.com*

INTRODUCTION

Against the backdrop of increasingly scarce global natural resources, solid wood furniture faces challenges such as high raw material costs and low sustainability (Deng *et al.* 2023). In contrast, panel furniture, primarily utilising wood-based panels, has gained increasing prominence in the furniture market due to its advantages: high raw material utilisation, low production costs, diverse styles, and suitability for large-scale manufacturing. An ever-growing number of consumers and manufacturers are opting for panel furniture, gradually establishing it as a viable alternative to solid wood furniture (Han *et al.* 2022).

The primary raw materials for panel furniture are various wood-based panels, with medium-density fibreboard and particleboard being the most prevalent (Huang *et al.* 2022). These panels utilise wood particles as their base material, bonded together through adhesive pressing. As the wood particles are present in a largely dispersed state, their cohesion relies primarily on adhesive bonding, resulting in significantly lower strength compared to the natural interlocking of continuous fibres in solid timber (Ding *et al.* 2022). Consequently, when wood-based panels bear loads, stresses cannot be effectively

transmitted along long fibres as effectively as in solid timber. This leads to stress concentration at the interfaces between particles and adhesive, potentially causing fractures. This material characteristic results in generally poor bending performance for wood-based panels (Banjo *et al.* 2022). Under prolonged loading, they are prone to deformation or even failure, compromising the structural reliability of furniture (Li *et al.* 2023).

Taking shelves within cabinet furniture as an example, as the primary load-bearing components, they endure multiple loads from books and items during use, operating under complex stress conditions that render them susceptible to bending deformation (Wang *et al.* 2023). Such deformation not only compromises the furniture's visual appeal but also significantly reduces its service life (Liu *et al.* 2021).

Polyamide (PA) stands as an engineering plastic renowned for its outstanding comprehensive properties and extensive applications. Compared to materials such as acrylonitrile-butadiene-styrene (ABS) and polylactic acid (PLA), it exhibits superior rigidity, toughness, and wear resistance (Feng *et al.* 2022). Polyamide 6 (PA6) represents one of the most extensively employed categories within the polyamide family. As a semi-crystalline polymer, its outstanding mechanical properties and favourable processability have established it as one of the most favoured high-performance 3D printing filaments currently available on the market (Li *et al.* 2022). This study utilized fused filament fabrication (FFF) technology and PA6 filament to produce structurally safe and reliably performing 3D-printed shelf reinforcers through customized structural design and printing process optimization. These reinforcers not only enhance the shelves' bending performance and load-bearing capacity, thereby extending the furniture's service life, but also demonstrate the application advantages of 3D printing technology in the production of customised household items.

EXPERIMENTAL

Materials

The PA6 filament (Blue, 1.75 mm diameter, Miracle 3D, Suzhou, China) with a density of 1.15 g/cm^3 and a melting point of 250 °C was employed for additive manufacturing *via* FFF technology (Yang *et al.* 2022).

Specimen Preparation

Referring to the standard ISO 178-2019, a rectangular specimen (length of 160 mm, width of 15 mm, thickness of 8 mm) was designed in SolidWorks software (Education version 2016, Dassault Systemes, Paris, France). The additive manufacturing of the rectangular specimen was completed using an industrial-grade FFF 3D printer (X-Y-Z printing, 0.4 mm nozzle diameter, Miracle 3D, Suzhou, China) and PA6 filament. The general process parameters of the 3D printer were set as follows: extrusion temperature (250 °C), print speed (50 mm/s), extrusion extent (100%), layer height (0.2 mm), and infill density (50%). Additionally, this study selected three process parameters (infill structure, infill thickness, and extrusion flow rate) that significantly influence the bending performance of 3D-printed PA6 models for single-factor experiments (Mo *et al.* 2022). A total of 15 specimens were prepared for each single-factor experiment group.

Performance Test

The bending performance of the rectangular specimens was tested using the three-point bending method at a room temperature of 20 °C, with the testing apparatus shown in Fig. 1. The specific test procedure was as follows: First, the rectangular specimen was placed on the two supports of the three-point bending fixture, with the support span set to 120 mm. Subsequently, the universal testing machine (AG-X, 20 kN, Shimadzu, Kyoto, Japan) was activated to apply a bending load at a rate of 2 mm/min until the specimen fractured. The maximum load at the point of fracture was recorded, and the bending strength of the specimen was calculated based on this maximum load. The elastic modulus was determined by calculating the slope of the linear elastic segment of the force-deflection curve (Wang *et al.* 2022).

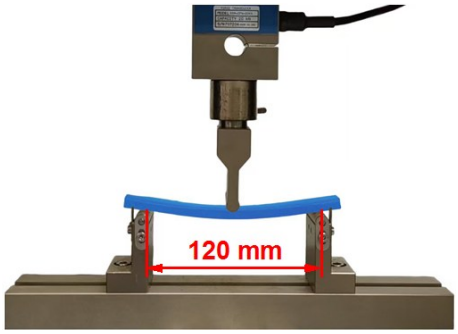

Fig. 1. Three-point bending method

RESULTS AND DISCUSSION

Effect of Infill Structure on the Bending Performance of PA6 Models

The infill thickness was set to 1.2 mm and the extrusion flow rate to 15 mm^3/s. The bending performance of 3D-printed PA6 models featuring honeycomb, grid, and line infill structures (as shown in Fig. 2) was tested, and the test results are shown in Fig. 3. As evident from Fig. 3, the PA6 model printed with the honeycomb infill structure exhibited the highest bending strength and elastic modulus, demonstrating the best bending performance. The grid infill structure yielded the second-best bending performance, while the line infill structure performed the worst. This occurs because the line infill structure possesses a relatively singular stress transmission pathway. When the model undergoes bending loads, stresses primarily propagate parallel to the infill walls, readily concentrating at interlayer bonding zones and consequently inducing interlayer shear failure. In contrast, the honeycomb infill structure efficiently transmits stress along the infill wall direction through its hexagonal cells, achieving uniform stress distribution (Zhang *et al.* 2025). This structure also absorbs energy *via* plastic deformation of the infill walls until tensile failure or crushing occurs, exhibiting ductile failure characteristics (Qi *et al.* 2023). Whilst the grid infill structure possesses some stress dispersion capability, its structure contains numerous nodes (*i.e.*, intersections of infill walls). These nodes readily become stress concentration points under bending loads, often initiating microcracks or yielding first, thereby triggering overall model failure (Yu and Wu 2024). In summary, the PA6 model printed with a honeycomb infill structure exhibits the most favourable bending performance.

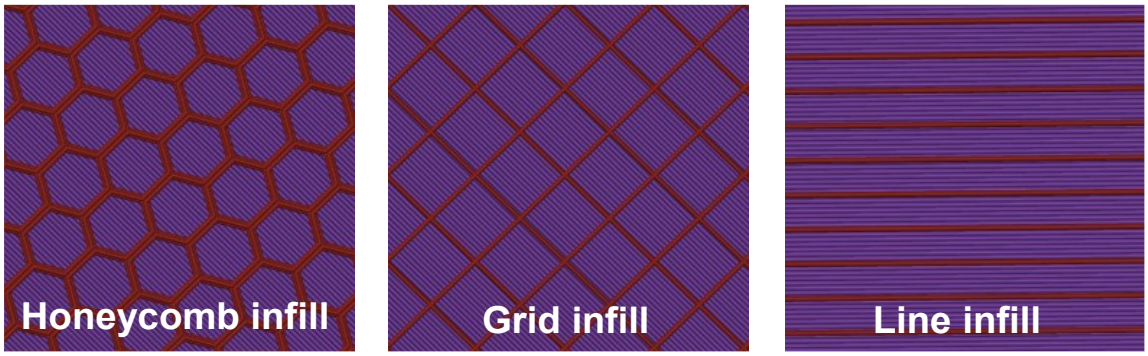

Fig. 2. Schematic diagram of infill structures

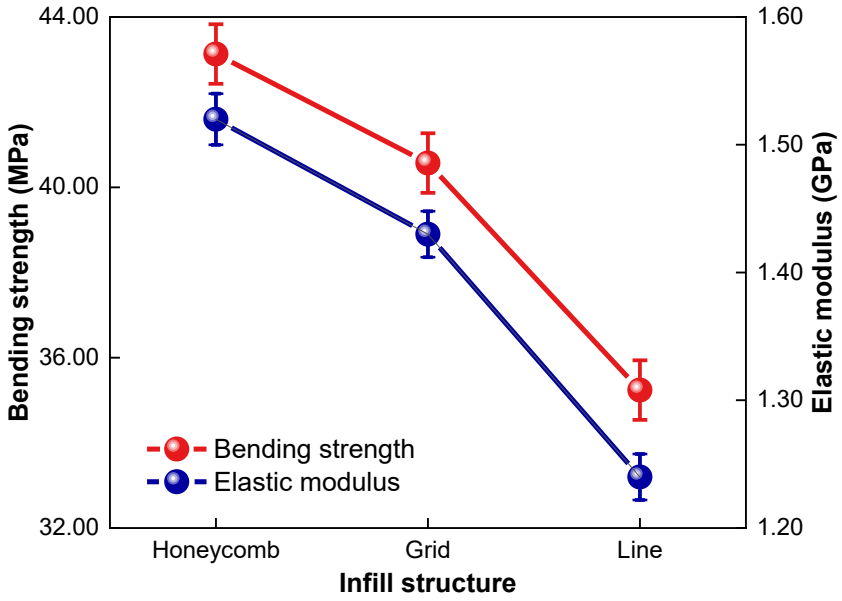

Fig. 3. Effect of infill structure on the bending performance of PA6 models

Effect of Infill Thickness on the Bending Performance of PA6 Models

The infill structure was set to honeycomb and the extrusion flow rate to 15 mm³/s. The bending performance of 3D-printed PA6 models with three infill thicknesses (0.4, 0.8, and 1.2 mm) was tested, and the test results are shown in Fig. 4. Both the bending strength and elastic modulus of the PA6 models increased with the increase of infill thickness, indicating a gradual enhancement in bending performance. This occurred because the effective load-bearing area of the PA6 models correspondingly increased with the increase of infill thickness, thereby reducing the stress distributed per unit area and consequently strengthening the PA6 models' resistance to bending failure (Liu *et al.* 2025). Furthermore, infill structures with thinner walls are prone to instability and buckling under load. Increasing wall thickness significantly improves the stability of the infill structure, enabling it to buckle under higher load conditions (Chen *et al.* 2022). In summary, increasing the infill thickness is beneficial for enhancing the bending performance of 3D-printed PA6 models.

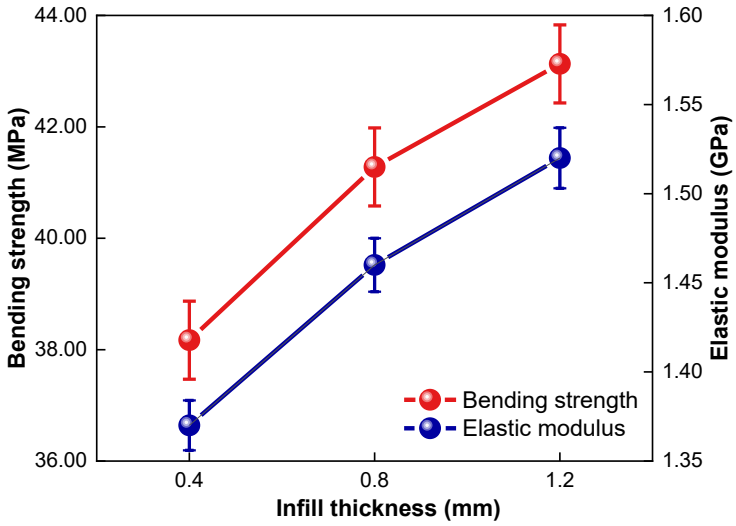

Fig. 4. Effect of infill thickness on the bending performance of PA6 models

Effect of Extrusion Flow Rate on the Bending Performance of PA6 Models

The infill structure was set to honeycomb and the infill thickness to 1.2 mm. The bending performance of 3D-printed PA6 models with three extrusion flow rates (8, 10, and 12 mm^3/s) was tested, and the test results are shown in Fig. 5. Both the bending strength and elastic modulus of the PA6 models increased with the increase of extrusion flow rate, indicating a gradual enhancement in bending performance. With the increase of extrusion flow rate, more molten PA6 filaments flow under the action of surface tension, filling the gaps in the structure (Hu *et al.* 2021). However, under the nozzle extrusion pressure, the molten PA6 filaments are thoroughly compressed at the interlayer bonding interfaces. This increases the contact area between adjacent layer filaments, promoting mutual diffusion and entanglement of PA6 molecular chains (Hang *et al.* 2025). Consequently, the interlayer bonding strength of PA6 models is enhanced, thereby strengthening the PA6 models' resistance to bending failure. In summary, increasing the extrusion flow rate is beneficial for enhancing the bending performance of 3D-printed PA6 models.

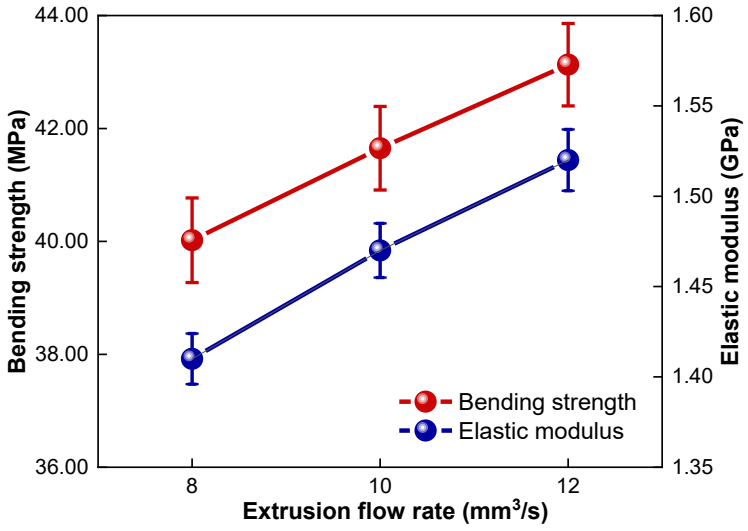

Fig. 5. Effect of extrusion flow rate on the bending performance of PA6 models

3D Modelling

The primary step in manufacturing furniture shelf reinforcers using FFF technology and PA6 filament involves precise 3D modelling. This study employed SolidWorks software to custom design the reinforcer based on the target shelf's thickness and length dimensions. As shown in Fig. 6, the cross-section of this reinforcer is designed in a 'U' shape. It is installed by embedding it into the shelf's edge banding and securing it to the shelf's side *via* self-tapping screws. Leveraging its own rigidity, the reinforcer effectively assists the shelf in sharing bending loads, thereby significantly suppressing bending deformation.

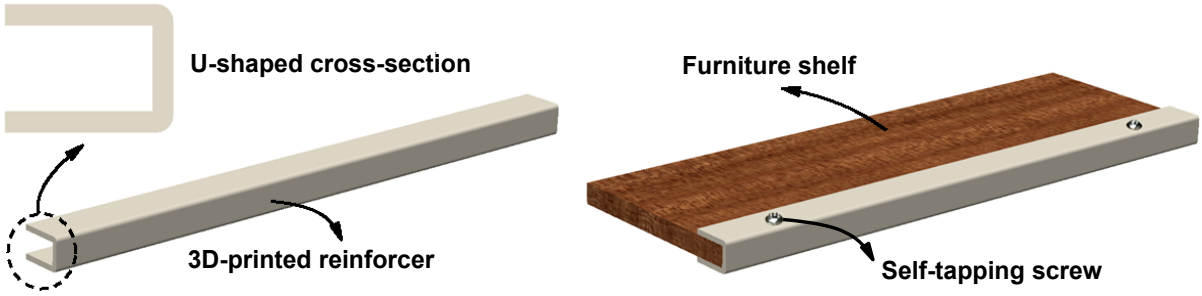

Fig. 6. 3D model of furniture shelf reinforcer

Slicing

The critical task in 3D printing slicing involves setting process parameters. Based on the single-factor experiments described above, the optimal process parameters were determined: the infill structure was set to honeycomb, the infill thickness to 1.2 mm, and the extrusion flow rate to 12 mm^3/s. Furthermore, to balance the mechanical properties of the reinforcer with material costs, printing time, and other factors, the remaining process parameters were set as follows: layer height (0.2 mm), extrusion temperature (250 °C), print speed (50 mm/s), hot bed temperature (70 °C), and infill density (50%). When adjusting the reinforcer's printing orientation, the layer bonding surfaces must be positioned perpendicular to the primary stress direction to prevent interlayer brittle fracture under load (Hu *et al.* 2024).

3D Printing

The shelf reinforcer was additively manufactured using an industrial-grade FFF 3D printer and PA6 filament. After printing, the surface of the reinforcer was sanded to ensure precise fitting with the shelf. Finally, the 3D-printed shelf reinforcer was secured to the shelf sides using self-tapping screws, with the installation effect shown in Fig. 7. This 3D-printed shelf reinforcer demonstrated good surface quality and is custom-designed based on the dimensions of the furniture shelf to ensure a tight fit. It not only significantly enhances the shelf's bending performance and load-bearing capacity, effectively extending the furniture's service life, but also exemplifies the customization advantages of 3D printing technology, providing practical reference for the rapid development of similar household items.

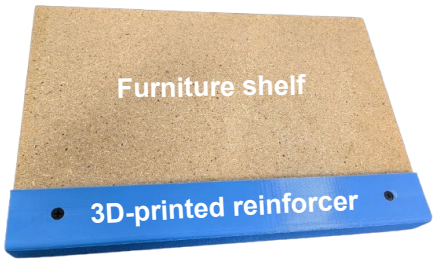

Fig. 7. 3D-printed prototype of the furniture shelf reinforcer

Comparative Experiment

A comparative bending performance experiment was conducted on shelves with and without reinforcers installed. The experiment utilised eight identical particleboards (length of 40 mm, width of 20 mm, thickness of 1.8 mm), four fitted with reinforcers and four without. Considering that shelves in cabinet furniture typically employ corner brackets, metal pins, or round dowels as lateral supports, all such support methods can be simplified into simply supported beam mechanical models. Consequently, a simply supported beam apparatus (as shown in Fig. 8) was utilised for this experiment. A 200 N load was applied centrally to each shelf to simulate the actual stress conditions imposed by items such as books. A dial gauge was positioned beneath the central underside of each shelf to measure deflection. After 24 hours of loading, the deflection values for each shelf were recorded, with results shown in Fig. 9. As evident from Fig. 9, shelves fitted with the reinforcers exhibited significantly lower deflection than those without, demonstrating the structural enhancement efficacy of these 3D-printed shelf reinforcers.

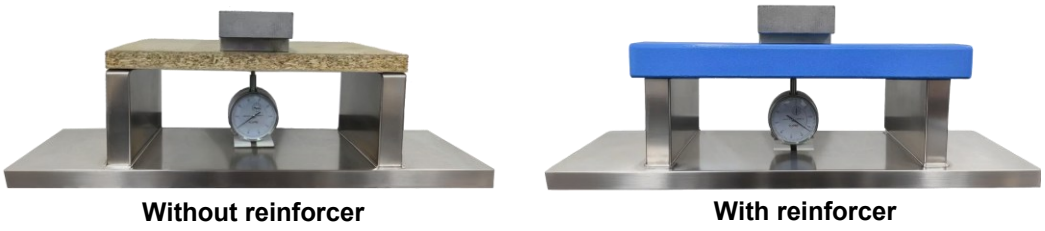

Fig. 8. Comparative bending performance experiment

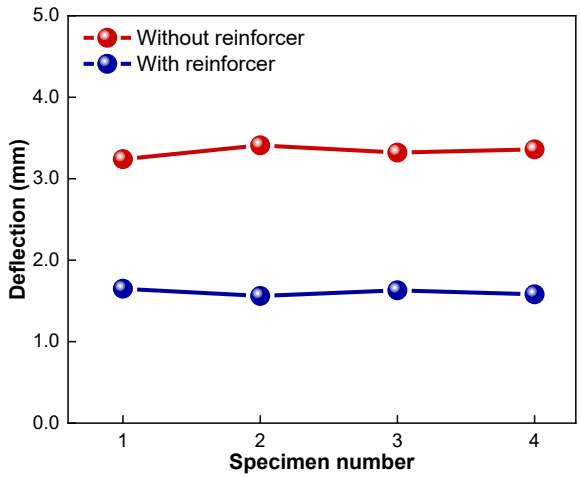

Fig. 9. Comparison of deflection values

CONCLUSIONS

1. This study analysed the bending performance of PA6 models under varying process parameters (infill structure, infill thickness, and extrusion flow rate) using the three-point bending method. Experimental results indicate that among the three infill structures, the honeycomb infill structure exhibited the best bending performance, followed by the grid infill structure, while the line infill structure demonstrated the worst bending performance. As both infill thickness and extrusion flow rate increased, the bending performance of the PA6 models progressively improved.
2. This study developed a 3D-printed shelf reinforcer using PA6 filament based on FFF technology. The reinforcer effectively enhances the shelf's bending performance and load-bearing capacity, extending the furniture's service life and providing practical reference for the rapid development of similar household items.

REFERENCES CITED

Banjo, A. D., Agrawal, V., Auad, M. L.., and Celestine, A. N. (2022). "Moisture-induced changes in the mechanical behavior of 3D printed polymers," *Composites Part C: Open Access*, 2022(7), article 100243. https://doi.org/10.1016/j.jcomc.2022.100243

Chen, B.-R., Yu, X.-J., and Hu, W.-G. (2022). "Experimental and numerical studies on the cantilevered leg joint and its reinforced version commonly used in modern wood furniture," *BioResources* 17(3), 3952-3964. https://doi.org/10.15376/biores.17.3.3952-3964

Deng, J.-Z., Huang, N., and Yan, X.-X. (2023). "Effect of composite addition of antibacterial/photochromic/self-repairing microcapsules on the performance of coatings for medium-density fiberboard," *Coatings* 13(11), article 1880. https://doi.org/10.3390/coatings13111880

Ding, T.-T., Yan, X.-X., and Zhao, W.-T. (2022). "Effect of urea–formaldehyde resin–coated colour–change powder microcapsules on performance of waterborne coatings for wood surfaces," *Coatings* 12(9), article 1289. https://doi.org/10.3390/coatings12091289

Feng, X.-H., Yang, Z.-Z., Wang, S.-Q., and Wu, Z.-H. (2022). "The reinforcing effect of lignin-containing cellulose nanofibrils in the methacrylate composites produced by stereolithography," *Polymer Engineering and Science* 2022(9), 2968-2976. https://doi.org/10.1002/pen.26077

Han, Y., Yan, X.-X., and Zhao, W.-T. (2022). "Effect of thermochromic and photochromic microcapsules on the surface coating properties for metal substrates," *Coatings* 12(11), article 1642. https://doi.org/10.3390/coatings12111642

Hang, J.-Y., Zou, Y.-M., Yan, X.-X., and Li, J. (2025). "Preparation of thermochromic UV coating with urea-formaldehyde-coated ternary system on bleached poplar wood surface," *Coatings* 15(9), article 997. https://doi.org/10.3390/coatings15090997

Hu, W.-G., Li, S., and Liu, Y. (2021). "Vibrational characteristics of four wood species commonly used in wood products," *BioResources* 16(4), 7101-7111. https://doi.org/10.15376/biores.16.4.7101-7111

Hu, W.-G., Zhao, Y., Xu, W., and Liu, Y.-Q. (2024). "The influences of selected factors on bending moment capacity of case furniture joints," *Applied Sciences* 14(21),

article 10044. https://doi.org/10.3390/app142110044
Huang, N., Yan, X.-X., and Zhao, W.-T. (2022). "Influence of photochromic microcapsules on properties of waterborne coating on wood and metal substrates," *Coatings* 12(11), article 1750. https://doi.org/10.3390/coatings12111750
Li, S., and Hu, W.-G. (2023). "Study on mechanical strength of cantilever handrail joints for chair," *BioResources* 18(1), 209-219. https://doi.org/10.15376/biores.18.1.209-219
Li, W.-B., Yan, X.-X., and Zhao, W.-T. (2022). "Preparation of crystal violet lactone complex and its effect on discoloration of metal surface coating," *Polymers* 14(20), article 4443. https://doi.org/10.3390/polym14204443
Liu, Q., Gu, Y., Xu, W., Lu, T., Li, W., and Fan, H. (2021). "Compressive properties of green velvet material used in mattress bedding," *Applied Sciences* 11(23), article 11159. https://doi.org/10.3390/app112311159
Liu, Y., Li, J.-Y., and Hu, W.-G. (2025). "Aesthetic preferences of Minnan folk wooden altar table," *BioResources* 20(4), 10425-10446. https://doi.org/10.15376/biores.20.4.10425-10446
Mo, X.-F., Zhang, X.-H., Fang, L., and Zhang, Y. (2022). "Research progress of wood-based panels made of thermoplastics as wood adhesives," *Polymers* 14(1), article 98. https://doi.org/10.3390/polym14010098
Qi, Y.-Q., Sun, Y., Zhou, Z.-W., Huang, Y., Li, J.-X, and Liu, G.-Y. (2023). "Response surface optimization based on freeze-thaw cycle pretreatment of poplar wood dyeing effect," *Wood Research* 68(2), 293-305. https://doi.org/10.37763/wr.1336-4561/68.2.293305
Wang, L., Han, Y., and Yan, X.-X. (2022). "Effects of adding methods of fluorane microcapsules and shellac resin microcapsules on the preparation and properties of bifunctional waterborne coatings for basswood," *Polymers* 14(18), article 3919. https://doi.org/10.3390/polym14183919
Wang, Q., Feng, X.-H., and Liu, X.-Y. (2023). "Functionalization of nanocellulose using atom transfer radical polymerization and applications: A review," *Cellulose* 30, 8495-8537. https://doi.org/10.1007/s10570-023-05403-5
Yang, Z.-Z., Feng, X.-H., Xu, M., and Rodrigue, D. (2022). "Printability and properties of 3D printed poplar fiber/polylactic acid biocomposites," *BioResources* 16(2), 2774-2788. https://doi.org/10.15376/biores.16.2.2774-2788
Yu, S.-L., and Wu, Z.-H. (2024). "Research on the influence mechanism of short video communication effect of furniture brand: Based on ELM model and regression analysis," *BioResources* 19(2), 3191-3207. https://doi.org/10.15376/biores.19.2.3191-3207
Zhang, W.-J., Zou, Y.-M., Yan, X.-X., and Li, J. (2025). "Influence of two types of microcapsule composites on the performance of thermochromic UV coatings on bleached poplar wood surfaces," *Coatings* 15(9), article 1001. https://doi.org/10.3390/coatings15091001

Article submitted: September 26, 2025; Peer review completed: October 25, 2025; Revised version received: November 5, 2025; Accepted: November 6, 2025; Published: December 9, 2025.
DOI: 10.15376/biores.21.1.799-807